

SCIENTIFIC REPORTS



Correction: Publisher Correction

OPEN

miR-3140 suppresses tumor cell growth by targeting *BRD4* via its coding sequence and downregulates the *BRD4-NUT* fusion oncoprotein

Erina Tonouchi^{1,2}, Yasuyuki Gen¹, Tomoki Muramatsu¹, Hidekazu Hiramoto¹, Kousuke Tanimoto³, Jun Inoue¹ & Johji Inazawa^{1,4}

Bromodomain Containing 4 (*BRD4*) mediates transcriptional elongation of the oncogene *MYC* by binding to acetylated histones. *BRD4* has been shown to play a critical role in tumorigenesis in several cancers, and the *BRD4-NUT* fusion gene is a driver of NUT midline carcinoma (NMC), a rare but highly lethal cancer. microRNAs (miRNAs) are endogenous small non-coding RNAs that suppress target gene expression by binding to complementary mRNA sequences. Here, we show that *miR-3140*, which was identified as a novel tumor suppressive miRNA by function-based screening of a library containing 1090 miRNA mimics, directly suppressed *BRD4* by binding to its coding sequence (CDS). *miR-3140* concurrently downregulated *BRD3* by bind to its CDS as well as *CDK2* and *EGFR* by binding to their 3' untranslated regions. *miR-3140* inhibited tumor cell growth *in vitro* in various cancer cell lines, including *EGFR* tyrosine kinase inhibitor-resistant cells. Interestingly, we found that *miR-3140* downregulated the *BRD4-NUT* fusion protein and suppressed *in vitro* tumor cell growth in a NMC cell line, Ty-82 cells. Furthermore, administration of *miR-3140* suppressed *in vivo* tumor growth in a xenograft mouse model. Our results suggest that *miR-3140* is a candidate for the development of miRNA-based cancer therapeutics.

The bromodomain and extra-terminal domain (BET) family proteins, including *BRD2*, *BRD3*, *BRD4*, and *BRDT*, contain two conserved bromodomains that are associated with acetylated lysine in histones, facilitating transcriptional activation as epigenetic readers^{1,2}. Among the BET family proteins, *BRD4* has been shown to play a critical role in promoting tumor growth in several cancers, including acute myeloid leukemia^{3,4}, multiple myeloma⁵, *MLL*-fusion leukemia⁶, diffuse large B cell lymphoma⁷, triple negative breast cancer⁸, and pancreatic cancer⁹. *BRD4* is enriched at super-enhancers of several oncogenes, such as *MYC*, *CCND2*, and *BCL-XL*, in cancer cells, upregulating the transcription of these genes¹⁰. *BRD4* increases the transcription of the other oncogenes *BCL2*, *CDK6*, and *MYC* by binding to the chromatin locus of these genes and recruiting positive transcriptional elongation factor complex (P-TEFb) to the promoter¹¹. Thus, *BRD4* is thought to be a rational target for cancer therapy⁶.

NUT midline carcinoma (NMC) is a poorly differentiated carcinoma that arises in the midline of the upper aerodigestive tract or the mediastinum^{12,13}. NMC is rare, refractory to conventional treatments, and highly lethal, with a median survival period of 6.7–9.5 months^{12,13}. The pathogenesis of NMCs involves the *BRD4-NUT* fusion gene, which is caused by a unique chromosome translocation t(15; 19)(q13; p13.1) in the majority of cases, although *BRD3-NUT* fusion by a t(9; 15)(q34; q14), *NSD3-NUT* fusion by a t(8; 15)(p12; q15), and *ZNF532-NUT* fusion by a t(15; 18)(q14; q23) occur in the remaining few cases^{13–15}. The translocation breakpoints occur within intron 10 of the *BRD4* gene (19p13.1) and intron 2 of *NUT* (15q14), such that the *BRD4-NUT* protein contains

¹Department of Molecular Cytogenetics, Medical Research Institute, Tokyo Medical and Dental University, Tokyo, Japan. ²Department of Maxillofacial Surgery, Graduate School, Tokyo Medical and Dental University, Tokyo, Japan. ³Genome Laboratory, Medical Research Institute, TMDU, Tokyo, Japan. ⁴Bioresource Research Center, Tokyo Medical and Dental University, Bunkyo-ku, Tokyo, Japan. Correspondence and requests for materials should be addressed to J.I. (email: johinaz.cgen@mri.tmd.ac.jp)

both acetyl-histone binding bromodomains and the extraterminal domain of BRD4 (i.e., the full functional domain of BRD4)¹³. The BRD4-NUT oncoprotein promotes tumor cell growth through the function of BRD4 as well as that of NUT^{16–18}.

The first-generation BET bromodomain inhibitor JQ1 binds to the acetyl-lysine binding pocket of BRD4, and thus, JQ1 depletes not only BRD4 but also BRD4-NUT from chromatin by preventing the binding of BRD4 to chromatin^{17,19}. As a result, JQ1 inhibits BRD4-mediated transcription of oncogenes, such as *MYC*^{8,20,21}. Several studies have shown that BET bromodomain inhibitors are highly effective against various intractable cancers, including triple negative breast cancer⁸, pancreatic cancer⁹, and NMC²², although resistance to BET bromodomain inhibition can be acquired through various mechanisms^{8,23}. Several clinical trials using BET bromodomain inhibitors have been started^{16,24–26}.

microRNAs (miRNAs) are endogenous small non-coding RNAs of 20–25 nucleotides that decompose or inhibit protein translation of mRNA by binding to complementary mRNA sequences^{27,28}. An individual miRNA has multiple target genes, and an individual gene can be targeted by multiple miRNAs²⁸. Although many studies have revealed that miRNAs repress gene expression by binding to 3' untranslated regions (3'UTR) of mRNAs, an increasing body of evidence supports that miRNAs also bind to the coding sequences (CDS) of target mRNAs and that miRNA binding to the CDS of mRNAs can effectively suppress translation^{29–31}. Our previous study also revealed that *miR-432-3p* directly targets *KEAP1* via its CDS³².

Because a single miRNA can simultaneously repress numerous target genes, miRNA mimics targeting several oncogenes may be useful as therapeutic agents for cancer therapy³³. In the present study, to investigate the novel candidate miRNAs for the development of miRNA-based cancer therapeutics, we conducted function-based screening using a miRNA library containing 1090 miRNAs. We revealed that *miR-3140*, identified as a novel tumor suppressive miRNA (TS-miRNA), repressed BRD4 directly by binding to its CDS. Furthermore, we showed that *miR-3140* also downregulated the BRD4-NUT oncoprotein in NMC cells. *miR-3140* suppresses other tumor promoting genes, such as *EGFR* and *CDK2*, via 3'UTR. Finally, the effects of *miR-3140* on tumor growth were tested *in vivo*.

Results

***miR-3140* was identified as a novel TS-miRNA by function-based miRNA library screening.** To extract novel TS-miRNAs, we performed function-based miRNA library screening from a library containing 1090 miRNA mimics in Panc1 cells. The strategy and brief results of this study are shown in Fig. 1a. In this study, the relative cell growth ratio was determined after transfection of each miRNA in two Panc1-derived clones, PEGadZsG-Panc1 #1 and #2 cells, which were established in our previous study³⁴. Figure 1b shows the results of this screening in Panc1 #1 (left) and #2 (right) 72 hours after transfection with each miRNA. We set the criteria for extracting TS-miRNAs (cell growth ratio < 0.6), and then extracted 29 miRNAs from Panc1 #1 and 65 miRNAs from Panc1 #2 cells, respectively (Fig. 1c). Twelve miRNAs that inhibited cell growth in both screening assays were identified as candidate TS-miRNAs (Table 1)^{35–38}. Then, 4 miRNAs were extracted according to annotation confidence, which means the certainty of the actual existence of a particular miRNA, determined using miRBase (<http://www.mirbase.org/>)³⁹. Among these 4 miRNAs, little is known about the tumor-suppressive function of *miR-3140*. Thus, we focused on a detailed analysis of *miR-3140*.

***miR-3140* inhibited *in vitro* tumor cell growth in various cancer cell lines.** To confirm the growth suppressive effect of *miR-3140* observed in the function-based screening, we evaluated the cell proliferation *in vitro* after transfection with *miR-3140* or *miR-NC* in two pancreatic cancer cell lines, Panc1 and MIA PaCa2 cells, respectively. Consistent with the screening results, overexpression of *miR-3140* significantly inhibited tumor cell growth in both cell lines (Fig. 1d,e). We next investigated whether *miR-3140* suppresses *in vitro* tumor cell growth in various cell lines including triple negative breast cancer (MDA-MB-231), esophageal cancer (KYSE150), liver cancer (Sk-Hep1), and non-small-cell lung carcinoma (HUT29 and A549). We also tested the effects of *miR-3140* in KYSE150 CDDP-R cells, which are resistant to cisplatin³⁶. As shown in Fig. 1e, overexpression of *miR-3140* markedly reduced tumor cell growth in all the cancer cell lines we tested. Taken together, *miR-3140* inhibited *in vitro* tumor cell growth.

***miR-3140* repressed *CDK2* and *EGFR* through 3'UTR interactions.** To investigate genes downregulated by *miR-3140*, gene expression array analysis was performed in three cancer cell lines, Panc1, MIA PaCa2, and MDA-MB-231 cells. As shown in a Venn diagram (Fig. 2a, left), the expression levels of 228 genes decreased by more than 2-fold in *miR-3140*-transfected cells compared with *miR-NC*-transfected cells. Among 228 genes, 99 genes were predicted to be direct targets of *miR-3140* according to the TargetScan program (<http://www.targetscan.org>) because candidate binding-sites for seed sequences of *miR-3140* exist in the 3'UTRs (Fig. 2a, right). Among the overlapping genes, we extracted *CDK2*, *CDK6*, and *EGFR*, which are all known to promote tumor cell growth^{40–42}. Western blotting showed that the protein levels of *CDK2*, *CDK6*, and *EGFR* were markedly reduced in *miR-3140*-transfectants of Panc1 and MIA PaCa2 cells, compared with *miR-NC*-transfectants (Fig. 2b). To determine whether *miR-3140* can directly bind to the 3'UTR of *CDK2*, *CDK6* and *EGFR*, we performed luciferase assays using reporter plasmid vectors containing the wild type (Wt) or mutant (Mt) 3'UTR of these genes in Panc1 cells. The luciferase activity of the Wt vectors, except for the 3'UTR of *CDK6* (Supplementary Fig. S1), was decreased compared with the empty vector (EV) in *miR-3140*-transfected cells and completely restored by the Mt vector for *CDK2* and *EGFR* (Fig. 2c). These results indicate that *CDK2* and *EGFR* are direct target genes of *miR-3140* through binding the 3'UTR region, although *CDK6* was downregulated indirectly by *miR-3140*.

To investigate whether *CDK2* and *EGFR* participate in the growth suppressive effects of *miR-3140*, we examined the cell proliferation *in vitro* after transfection with small interfering RNA (siRNA) targeting *CDK2*, *EGFR*, or negative control siRNA. As shown in Fig. 2d, *si-CDK2* significantly reduced tumor cell growth in MIA PaCa2

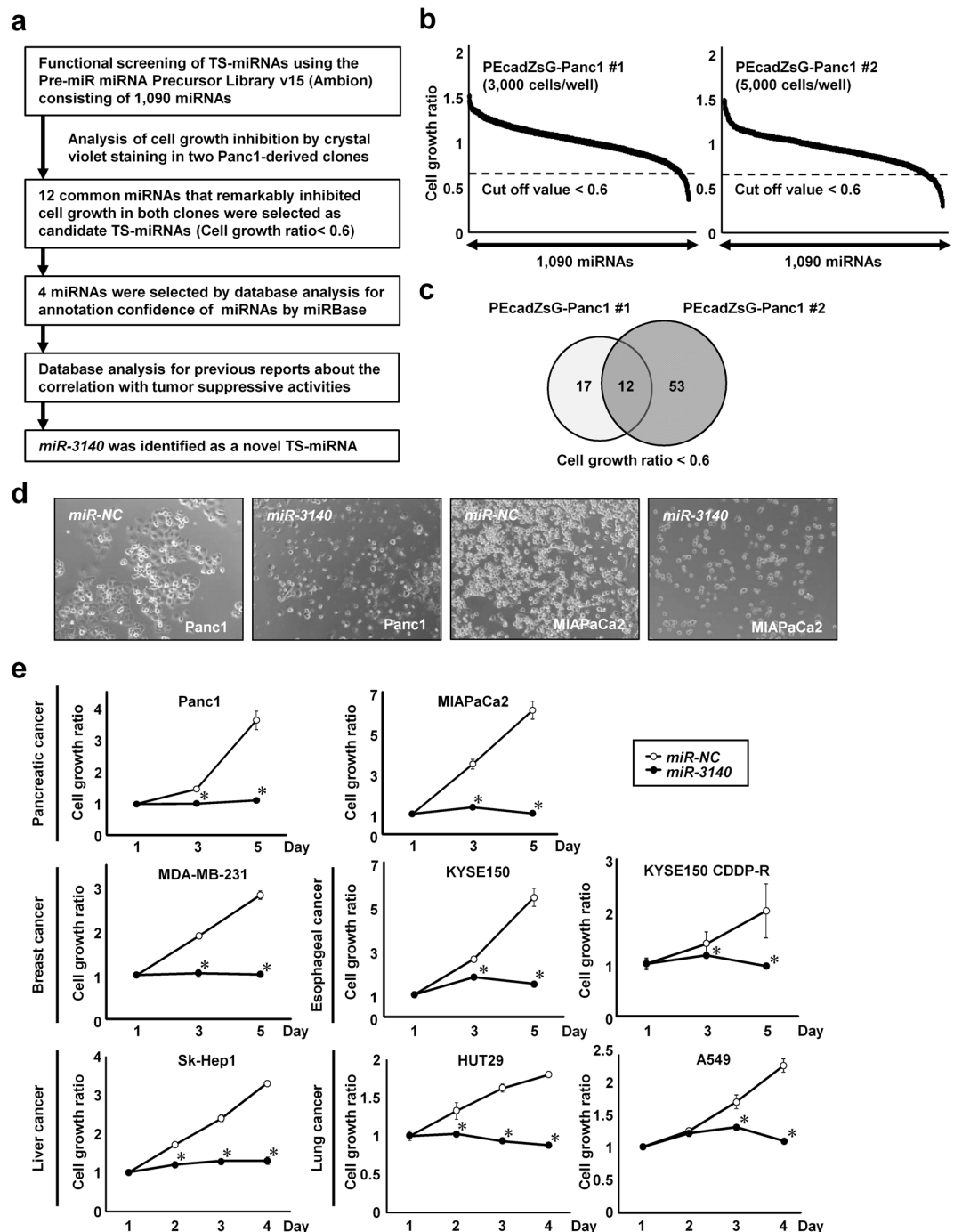


Figure 1. *miR-3140* was identified as a novel tumor suppressive miRNA (TS-miR) by function-based miRNA library screening. (a) The strategy used to identify novel TS-miRs in this study. (b) Results of function-based miRNA library screening in two Panc1-derived clones (PEcadZsG-Panc1 #1 and PEcadZsG-Panc1 #2 cells), using the Pre-miR miRNA Precursor Library-Human V15 consisting of 1,090 mature human miRNA mimics. The cell growth ratio was assessed with crystal violet staining using a relative ratio normalized based on the cell survival rate of cells transfected with negative control miRNA (*miR-NC*). A value of 0.6 was used to determine the cut-off value for growth inhibition (dotted line). (c) The Venn diagram showing the overlap of 12 miRNAs between Panc1 #1 (3000 cells/well) and #2 (5000 cells/well). (d) Phase contrast images of Panc1 and MIA PaCa2 cells transfected with 10 nmol/L of *miR-NC* or *miR-3140*. Images were obtained 3 days after transfection. (e) Cell growth assay in various types of cancer cells. Pancreatic cell lines (Panc1 and MIA PaCa2), a triple negative breast cancer cell line (MDA-MB-231), esophageal squamous cell carcinoma cell lines (KYSE150 and the cisplatin resistant cell line KYSE150 CDDP-R), a liver cancer cell line (Sk-Hep1), and non-small-cell lung cancer cell lines (HUT29 and A549) were transfected with 10 nmol/L of *miR-NC* or *miR-3140*. The cell growth ratio was assessed with the WST-8 assay based on the relative ratio compared with day 1. Bar, SD for triplicate experiments; * $P < 0.05$.

miRNA Precursor	Mature Sequence	Panc1 #1	Panc1 #2	Location	Host gene	Annotation Confidence (miRBase)	Ref [‡]
		Ratio [†]	Ratio [†]				
<i>hsa-miR-342-5p</i>	AGGGGUGCUAUCUGUGAUUGA	0.432	0.323	14q32.2	<i>EVL</i>	high	³⁵
<i>has-miR-449b*</i>	CAGCCACAACUACCCUGCCACU	0.357	0.446	5q11.2	<i>CDC20</i>		—
<i>hsa-miR-608</i>	AGGGGUGUGUUGGGACAGCUCGCGU	0.487	0.503	10q24.31	<i>SEMA4G</i>		³⁵
<i>hsa-miR-634</i>	AACCAGCACCCCAACUUUGGAC	0.443	0.579	17q24.2	<i>PRKA</i>		³⁶
<i>hsa-miR-671-3p</i>	UCCGGUUCUCAGGGCUCCACC	0.563	0.467	7q36.1	<i>CHPF2</i>	high	³⁷
<i>hsa-miR-876-3p</i>	UGGUGGUUACAAGUAAUUCA	0.407	0.439	9p21.1	<i>LINGO2</i>	high	³⁸
<i>hsa-miR-1289</i>	UGGAGUCCAGGAAUCUGCAUUUU	0.576	0.338	20q11.22	<i>GDF5</i>		—
				5q31.1	<i>FSTL4</i>		
<i>hsa-miR-1293</i>	UGGUGUGUCUGGAGAUUUGUGC	0.580	0.425	12q13.12	<i>LIMA1</i>		—
<i>hsa-miR-3126-3p</i>	CAUCUGGCAUCCGUCACACAGA	0.582	0.533	2p13.3	<i>ANTXR1</i>		—
<i>hsa-miR-3140</i>	AGCUUUUGGAAUUCAGGUAGU	0.508	0.459	4q31.3	<i>FBXW7</i>	high	—
<i>hsa-miR-3165</i>	AGGUGGAUGCAAUGUGACCUCA	0.533	0.370	11q13.4	<i>NUMA1</i>		—
<i>hsa-miR-3173</i>		0.551	0.372	14q32.13	<i>DICER1</i>		—

Table 1. Summary of 12 miRNAs selected as candidates for novel tumor suppressive miRNAs in functional based screening with Pre-miR miRNA Precursor Library v15. [†]Ratio means the cell growth ratio of viable cells as assessed by crystal violet staining 72 hours after transfection with miRNAs, relative to the control transfectants. [‡]Reference is TS-miRNA.

cells, but not in Panc1 cells. Similarly, *si-EGFR* suppressed cell proliferation in Panc1 cells (Fig. 2e), but not in MIAPaCa2 cells (Supplementary Fig. S2). These results suggested that *CDK2* and *EGFR* contribute to tumor cell growth in a cell-dependent manner. Thus, downregulation of *CDK2* and *EGFR* may partially contribute to *miR-3140*-mediated suppression of tumor cell growth.

***miR-3140* suppressed tumor cell growth in EGFR tyrosine kinase inhibitor (EGFR-TKI)-resistant lung cancer cells.** Since *miR-3140* directly targeted *EGFR*, we next examined whether *miR-3140* overcame the resistance to EGFR-TKIs. *EGFR* is one of the most frequently mutated “driver” genes in non-small cell lung carcinoma (NSCLC) and EGFR-TKIs are used for the treatment of *EGFR*-mutated-NSCLC. Therefore, we examined the effects of *miR-3140* in *EGFR*-mutated-NSCLC cells. In agreement with past reports, HUT29 cells, which harbor the *EGFR* L858R mutation, were sensitive to the EGFR-TKIs gefitinib and erlotinib, whereas NCI-H1975 cells, which harbor the *EGFR* L858R/T790M double mutation, were resistant to gefitinib and erlotinib (Supplementary Fig. S3a,b)⁴³. Both *miR-3140* and *si-EGFR* reduced the expression of *EGFR* in NCI-H1975 cells, resulting in the suppression of *in vitro* tumor cell growth in NCI-H1975 cells (Fig. 2e,f). These results suggested that *miR-3140* may overcome the acquired resistance to EGFR-TKIs at least in part by suppressing mutant *EGFR* in NSCLC cells.

Suppression of BET family genes inhibited tumor cell growth. Because the effects of *miR-3140* on *in vitro* tumor cell growth were much greater than those of *si-CDK2* and *si-EGFR* (Figs 1e and 2d–f), concurrent downregulation of additional target genes may be necessary for the induction of *miR-3140*-mediated inhibition of tumor cell growth. A growing body of evidence suggested that coding sequence (CDS) of mRNA could be directly targeted by a miRNA-containing RISC complex^{29–31}. Thus, we explored additional target genes of *miR-3140* using the STarMirDB database (<http://sfold.wadsworth.org>)⁴⁴, which predicts miRNA target genes based on CDS binding. Among the 228 genes downregulated by *miR-3140* in 3 cell lines (Fig. 2a), candidate binding-sites for the seed sequence of *miR-3140* exist in the CDS of 103 genes (Fig. 3a, Supplementary Table S1). From these 103 overlapping genes, we extracted *BRD4* as a candidate target gene of *miR-3140*, because *BRD4* has been shown to play a critical role in promoting tumor growth in several cancers through upregulates the transcription of oncogenes, including *MYC* and *CCND2*. Our gene expression array analysis showed that *miR-3140* downregulated the expression of *MYC* and *CCND2* as well as *BRD4* in Panc1 cells, suggesting that *BRD4* plays a critical role for tumor cell growth in Panc1 cells. As shown in Fig. 3b, *miR-3140* markedly reduced *BRD4* protein expression. Furthermore, we found that other BET family genes, *BRD2* and *BRD3*, together with genes for the downstream signaling pathways of *BRD4*, *MYC*, phosphorylated *STAT3* and *Cyclin D2*^{10,20}, were significantly reduced by *miR-3140* (Fig. 3b). Transfection of siRNA targeting each BET family gene, especially *si-BRD4*, markedly inhibited tumor cell growth (Fig. 3c, Supplementary Fig. S4). Conversely, overexpression of *BRD4* promoted cell proliferation compared to transfection with an empty vector (Fig. 3d). Taken together, downregulation of *BRD4* contributed to *miR-3140*-mediated suppression of tumor cell growth.

***miR-3140* repressed *BRD4* and *BRD3* by directly binding to the CDS region.** To examine whether *miR-3140* can directly bind to the CDS of *BRD4*, we first performed luciferase assays using reporter plasmid vectors containing Wt or Mt seed sequences in the CDS. Because two candidate binding-sites for the seed sequence of *miR-3140* exist within the CDS of *BRD4*, three mutant constructs (Mt1, Mt2 and Mt1 + 2) were established (Fig. 4a). The luciferase activity of the Wt vector was decreased compared with EV in *miR-3140* transfected cells and partially recovered with each Mt1 or Mt2 vector and completely restored with the Mt1 + 2 vector (Fig. 4a). We next examined whether *miR-3140* suppressed the expression of *BRD4* by binding to these positions within the

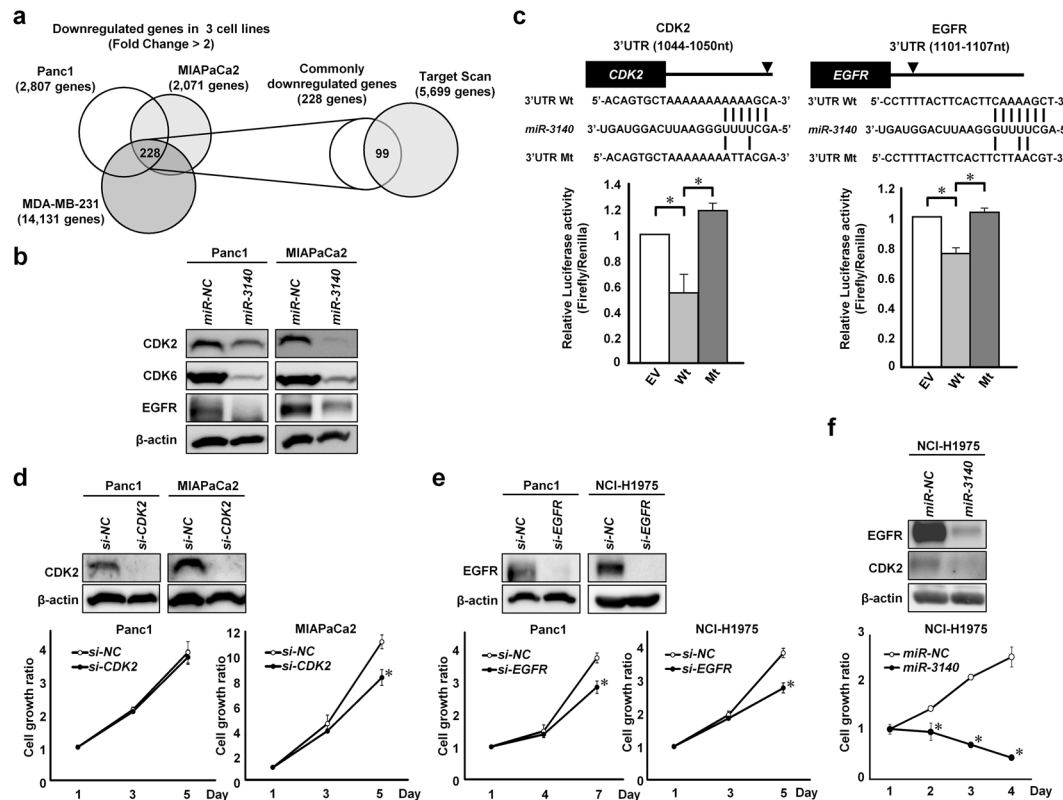


Figure 2. *miR-3140* targeted *CDK2* and *EGFR* by binding their 3'UTR regions. (a) Left, identification of downregulated genes after *miR-3140* transfection by a gene expression array. The Venn diagram shows that 228 genes were commonly downregulated (fold change >2) by transfection of *miR-3140* in Panc1, MIAPaCa2, and MDA-MB-231 cells. Right, prediction of candidate target genes regulated by *miR-3140* via their 3'UTR. The Venn diagram shows that 99 genes were predicted as candidate 3'UTR-targets of *miR-3140* by the TargetScan program. (b) Western blot analysis of *CDK2*, *CDK6*, and *EGFR* in Panc1 and MIAPaCa2 cells 72 hours after transfection with 10 nmol/L of *miR-NC* or *miR-3140*. (c) Luciferase reporter assays. Panc1 cells were transfected with the pmirGLO Dual Luciferase vectors containing wild type (Wt) *CDK2* and *EGFR* or mutant (Mt) 3'UTR target sites of these genes, and after 6 hours, either *miR-NC* or *miR-3140* was additionally transfected. Top, putative binding site of *miR-3140* within the 3'UTR of each gene and mutant sequences. Bottom, results of the luciferase assay; * $P < 0.05$. (d, e) Evaluation of the effect of *si-CDK2* or *si-EGFR*. Western blot analysis (top) and cell growth assay (bottom) in indicated cell lines after transfection with 20 nmol/L of negative control siRNA (*si-NC*) or siRNA targeting each gene. (f) Evaluation of the effect of *miR-3140* in EGFR-TKI-resistant lung cancer cells. Western blot analysis (top) and cell growth assay (bottom) in the indicated cell line after transfection with 10 nmol/L of *miR-NC* or *miR-3140*. Cell growth ratio was assessed with the WST-8 assay based on the relative ratio compared with day 1. Bar, SD for triplicate experiments; * $P < 0.05$.

CDS. Synonymous mutations were generated at each site of the Halotag-BRD4 protein (Supplementary Fig. S5a). Each of those Wt and Mt vectors were transfected into MIAPaCa2 cells followed by transfection of *miR-NC* or *miR-3140*, respectively. Whereas the expression level of exogenously expressed BRD4-Wt was reduced in the *miR-3140*-transfected cells, the *miR-3140*-induced reduction of exogenous BRD4 was restored by all three patterns of each mutation at binding-sites for the seed sequence of *miR-3140* (Fig. 4b). These combined data suggested that *miR-3140* can downregulate BRD4 expression by directly targeting its CDS.

Similarly, we examined whether *BRD3* was also a candidate target gene of *miR-3140*. Candidate binding-sites for the seed sequence of *miR-3140* exist within both the CDS and the 3'UTR of the *BRD3* gene. The luciferase activity of the 3'UTR-Wt vector did not decrease, but that of the CDS-Wt vector was decreased compared with EV in *miR-3140* transfectant, and this decrease was completely recovered by the CDS-Mt vector (Fig. 4c, d). Synonymous mutations were generated at the CDS site of the Halotag-BRD3 protein (Supplementary Fig. S5b). While the expression level of exogenously expressed BRD3-Wt was decreased in the *miR-3140*-transfected cells, this *miR-3140*-induced decrease in exogenous BRD3 was restored by the mutations at a binding-site for the seed sequence of *miR-3140* (Fig. 4e), suggesting that *miR-3140* can downregulate BRD3 expression by targeting its CDS as well as BRD4. Taken together, *miR-3140* targets *BRD4* and *BRD3* through their binding CDS regions.

***miR-3140* downregulated the BRD4-NUT fusion protein.** Based on the results that *miR-3140* directly targets the CDS of *BRD4*, we investigated whether *miR-3140* suppresses the *BRD4-NUT* fusion gene. The *BRD4-NUT* fusion is caused by t(15;19) translocation and drives NUT midline carcinoma (NMC), a rare,

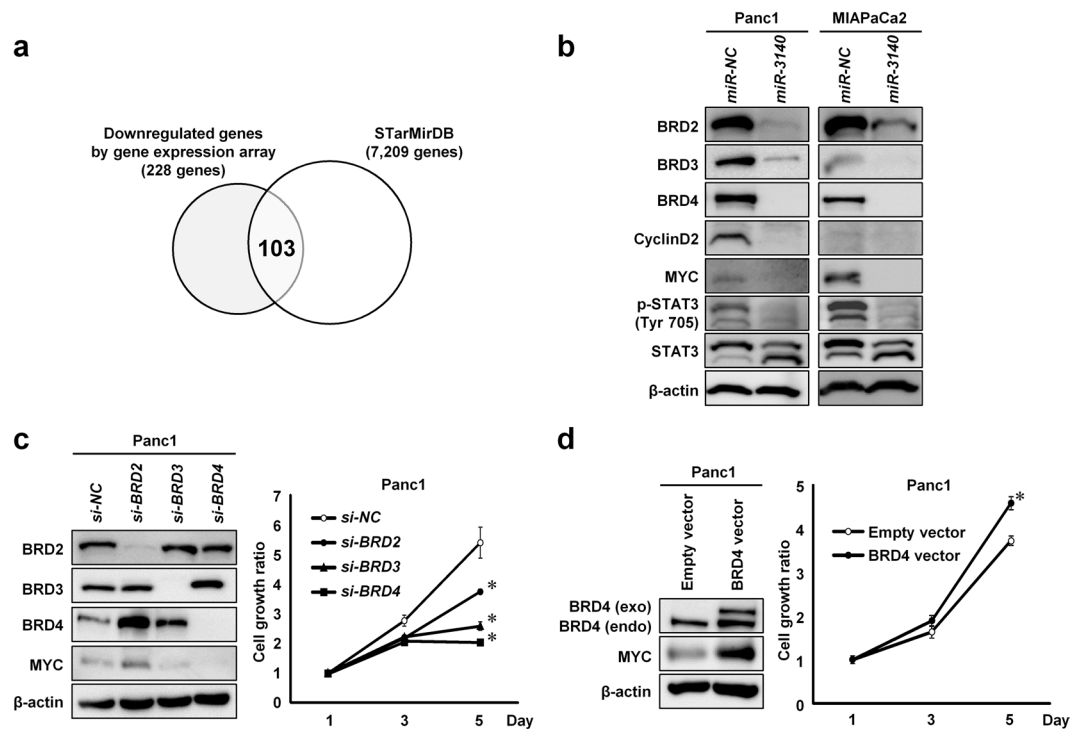


Figure 3. *miR-3140* downregulated BET family genes. **(a)** Prediction of candidate targets regulated by *miR-3140* via their coding sequences (CDS). The Venn diagram shows that 103 genes were predicted as candidate CDS-targets of *miR-3140* by the STarMirDB program. **(b)** Western blot analysis of BET family proteins (BRD2, BRD3, and BRD4) and downstream targets of BRD4 (Cyclin D2, MYC, and p-STAT3) in Panc1 and MIA PaCa2 cells 72 hours after transfection with 10 nmol/L of *miR-NC* or *miR-3140*. **(c,d)** Effects of knockdown of BET family proteins **(c)**, or overexpression of BRD4 **(d)** on cell growth in Panc1 cells. Cells were transfected with 20 nmol/L of *si-NC* or siRNA targeting BET family proteins **(c)**, and empty vector or BRD4-HaloTag expression vector **(d)**. Left, western blot analysis of indicated proteins in Panc1 cells 72 hours after transfection. Right, results of the cell growth assay. The cell growth ratio was assessed with the WST-8 assay based on the relative ratio compared with day 1. Bar, SD for triplicate experiments; * $P < 0.05$.

highly lethal cancer (Fig. 5a)¹². Consistent with past reports^{21,45}, JQ1 reduced MYC and significantly suppressed *in vitro* tumor growth of Ty-82 cells, a NMC cell line, which harbor t(15;19) bearing the BRD4-NUT fusion gene (Fig. 5b)⁴⁶. As shown in Fig. 5c, *miR-3140* repressed the expression of the BRD4-NUT fusion protein and its downstream target MYC in Ty-82 cells. As a result, *miR-3140* effectively suppressed *in vitro* tumor cell growth of Ty-82 cells (Fig. 5c).

Next, to test whether *miR-3140* can suppress tumor cell growth of JQ1-resistant cells, JQ1-resistant cells (Ty-82 JQ1-R) were generated from Ty-82 cells (IC₅₀: 0.43 μM in Ty-82 cells, 1.37 μM in Ty-82 JQ1-R cells; Fig. 5d). To determine whether Ty-82 JQ1-R cells have developed resistance by acquiring BRD4-NUT-dependence or not, we examined the effects of JQ1 in Ty-82 JQ1-R cells. The expression of MYC, a downstream effector of BRD4-NUT, was not suppressed sufficiently by JQ1 treatment in Ty-82 JQ1-R cells, whereas the expression of MYC was suppressed by JQ1 treatment in a dose-dependent manner in Ty-82 cells (Supplementary Fig. S6a). Knockdown of BRD4-NUT using RNA interference downregulated the expression of MYC and suppressed cell growth both in Ty-82 JQ1-R cells (Supplementary Fig. S6b). These results suggested that JQ1 could not block the effects of BRD4-NUT sufficiently in Ty-82 JQ1-R cells, although the mechanism is unknown. *miR-3140* downregulated the expression of BRD4-NUT fusion protein and MYC, and suppressed tumor cell growth in Ty-82 JQ1-R cells as well as Ty-82 cells (Fig. 5c,e). These combined data suggested that the resistance of JQ1 is, at least in part, dependence of BRD4-NUT/MYC pathway. Thus, our results suggested that *miR-3140* inhibited cell growth in Ty-82 JQ1-R cells by targeting BRD4-NUT.

***miR-3140* suppressed tumor growth in a xenograft mouse model.** We next examined the therapeutic effect of *miR-3140* through the local administration of dsRNA mimicking miRNA around MIA PaCa2-derived subcutaneous tumors in nude mice. *miR-NC* (left) or *miR-3140* (right) were administered into the subcutaneous space around tumors 5 times (7, 11, 15, 18, 21 days after the injection of MIA PaCa2 cells; Fig. 6a). Administration of miRNA did not produce any adverse consequences, such as body weight loss or local damage. As a result, tumors treated with *miR-3140* at 23 days after the injection of MIA PaCa2 cells were significantly smaller than tumors treated with *miR-NC* (Fig. 6b,c, Supplementary Fig. S7a,b). We confirmed that the expression of *miR-3140* was significantly high in the *miR-3140*-treated tumors compared to *miR-NC*-treated tumors by qRT-PCR (Fig. 6d). Furthermore, immunohistochemical staining showed that the expression of BRD4, BRD3, CDK2, and EGFR, the

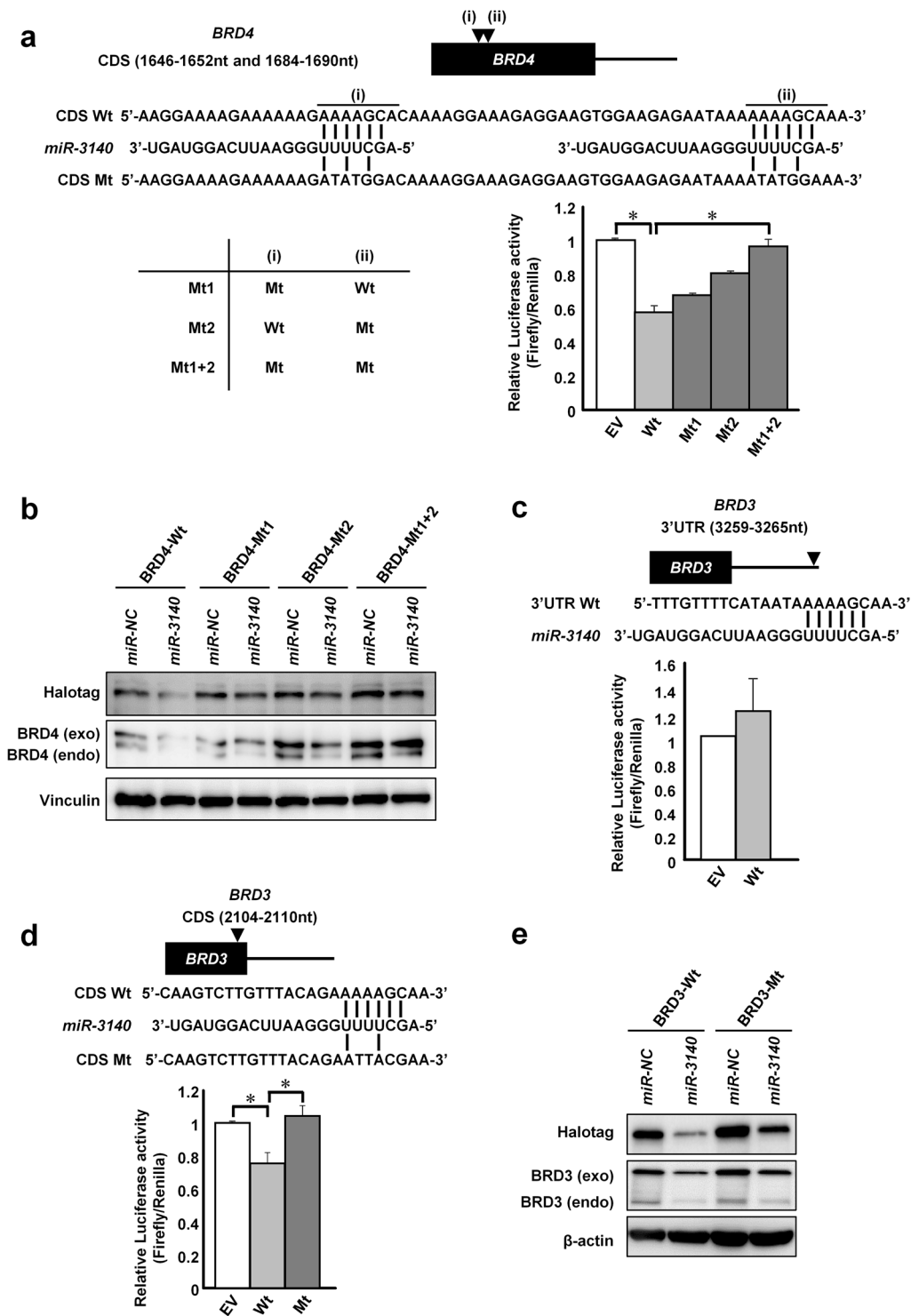


Figure 4. *miR-3140* directly targeted *BRD4* and *BRD3* by binding their coding regions. (a) Luciferase reporter assay. MIAPaCa2 cells were transfected with the pmirGLO Dual Luciferase vectors containing Wt or Mt *BRD4*, or empty vector (EV), and after 6 hours, either *miR*-NC or *miR-3140* was additionally transfected. Top, putative binding sequence of *miR-3140* within the CDS of *BRD4* and mutant sequences are indicated. Bottom, the results of luciferase assay; * $P < 0.05$. (b) Western blot analysis of *BRD4* in MIAPaCa2 cells. Cells were co-transfected with the Wt or Mt *BRD4* expression vector, and after 24 hours, either 10 nmol/L of *miR*-NC or *miR-3140* was additionally transfected. (c,d) Luciferase reporter assays. Panc1 cells were transfected with a reporter plasmid (Wt of *BRD3* 3'UTR or EV (c), or Wt, Mt of *BRD3* CDS or EV (d)) and after 6 hours, either *miR*-NC or *miR-3140* was additionally transfected. Top, putative binding sequences of *miR-3140* within the *BRD3* 3'UTR (c) and the *BRD3* CDS (d). Bottom, results of the luciferase assay; * $P < 0.05$. (e) Western blot analysis of *BRD3* in Panc1 cells. Cells were co-transfected with the Wt or Mt *BRD3* expression vector, and after 24 hours, either 10 nmol/L of *miR*-NC or *miR-3140* was additionally transfected.

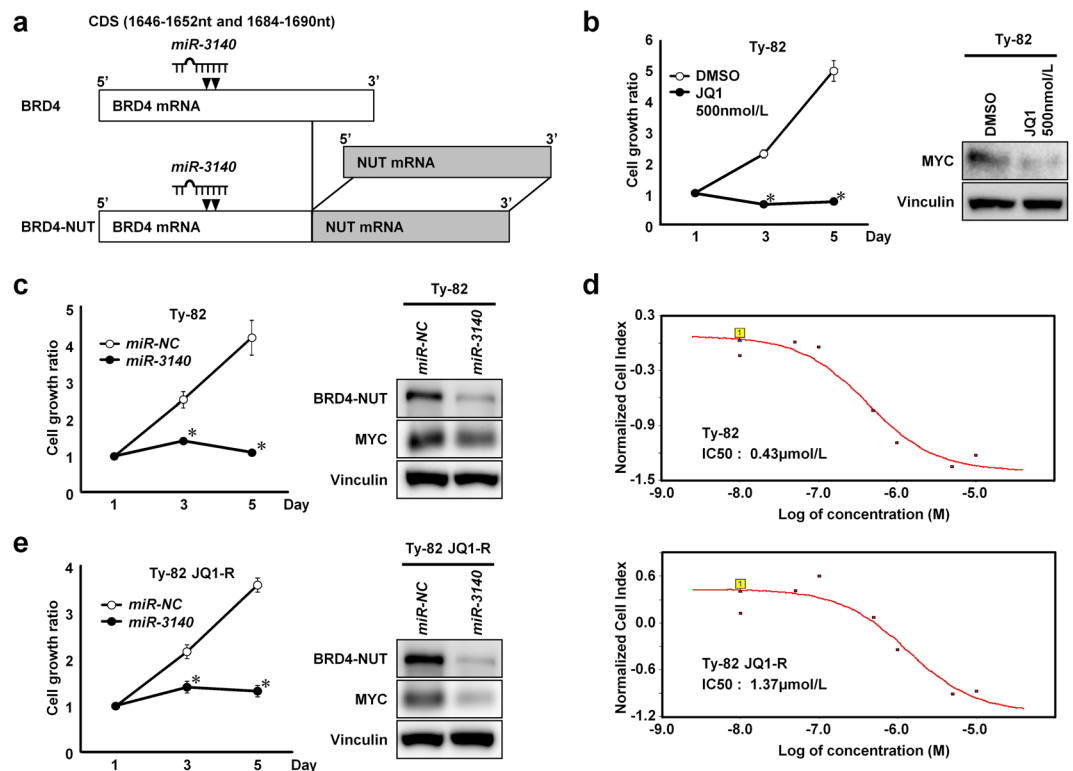


Figure 5. *miR-3140* downregulates the BRD4-NUT fusion protein. (a) Schema of the relationship between mRNA of the *BRD4-NUT* fusion gene in NUT midline carcinoma and the location of *miR-3140* target sites. (b) Effects of the BET bromodomain inhibitor JQ1 in Ty-82 cells. Left, the results of the cell growth assay. The cell growth ratio was assessed with the WST-8 assay based on the relative ratio compared with day 1. Bar, SD for triplicate experiments; * $P < 0.05$. Right, western blot analysis of MYC in Ty-82 cells 3 hours after transfection. (c,e) Left, cell growth assay in a NUT midline carcinoma cell line, Ty-82 (c) and its JQ1-resistant cells (Ty-82 JQ1-R) cells (e) which were transfected with 10 nmol/L of *miR-NC* or *miR-3140*. Cell growth ratio was assessed with the WST-8 assay based on the relative ratio compared with day 1. Bar, SD for triplicate experiments; * $P < 0.05$. Right, western blot analysis of the BRD4-NUT fusion protein and MYC in Ty-82 (c) and Ty-82 JQ1-R cells (e) 72 hours after transfection with 10 nmol/L of *miR-NC* or *miR-3140*. (d) Dose response curve of JQ1 for Ty-82 (upper) and Ty-82 JQ1-R cells (lower) at 50 hours following treatment with JQ1. Cell indexes were normalized with the last time point before JQ1 treatment.

targets of *miR-3140*, were reduced in the resected tumors treated with *miR-3140* (Fig. 6e, Supplementary Fig. S8). Although other targets of *miR-3140* may also participate in the tumor suppressive activity, *miR-3140* inhibited tumor growth *in vivo* at least in part by suppressing *BRD4*, *BRD3*, *CDK2* and *EGFR*.

Discussion

Here, we identified *miR-3140* as a novel TS-miRNA by function-based miRNA library screening. As summarized in Fig. 6f, we showed that *miR-3140* inhibited tumor cell growth in various cancer cells both *in vitro* and *in vivo* at least in part by directly targeting *BRD4*, *BRD3*, *CDK2*, and *EGFR*. Furthermore, we revealed that *miR-3140* suppressed the BRD4-NUT oncoprotein in NMC cells and that *miR-3140* inhibited *in vitro* tumor cell growth in NMC cells.

We revealed that *miR-3140* directly suppressed *EGFR* and *CDK2* via 3'UTR interaction. Both *EGFR* and *CDK2* play a role in cancer progression. *EGFR* is activated by gain-of-function mutations or amplification in several cancers including lung, head and neck, ovary, colon, and esophagus⁴³. Small molecule inhibitors, such as gefitinib and erlotinib, are used in lung cancer patients who have mutations on *EGFR*⁴³. We showed that *miR-3140* suppressed *in vitro* tumor cell growth by directly reducing *EGFR* expression in NCI-H1975 cells, which are *EGFR*-TKI resistant due to *EGFR* L858R/T790M double mutations^{43,47,48}. Although *in vivo* experiments are needed to confirm the effects of *miR-3140* on *EGFR*-TKI-resistant cells, our results suggest that *miR-3140* may overcome the acquired resistance to *EGFR*-TKIs in lung cancer. *CDK2* is another target of *miR-3140*. The catalytic activity of *CDK2*-CyclinE complexes is hyperactivated in several cancers by *Cyclin E* amplification, or a loss-of-function mutation of *FBXW7*, a ubiquitin ligase for *Cyclin E* degradation, although *CDK2* mutations are rare in human cancers⁴⁹. Thus, suppression of *CDK2* by *miR-3140* may contribute to the inhibition of tumor growth in some cancers.

Second, we identified that *miR-3140* suppressed *BRD4* and *BRD3* through binding to their CDS. Because BET bromodomain inhibitors suppressed BET family-mediated transcription of the oncogene *MYC*, they were reported to be promising agents for many cancers^{5,22}. Several BET inhibitors have entered into clinical trials in

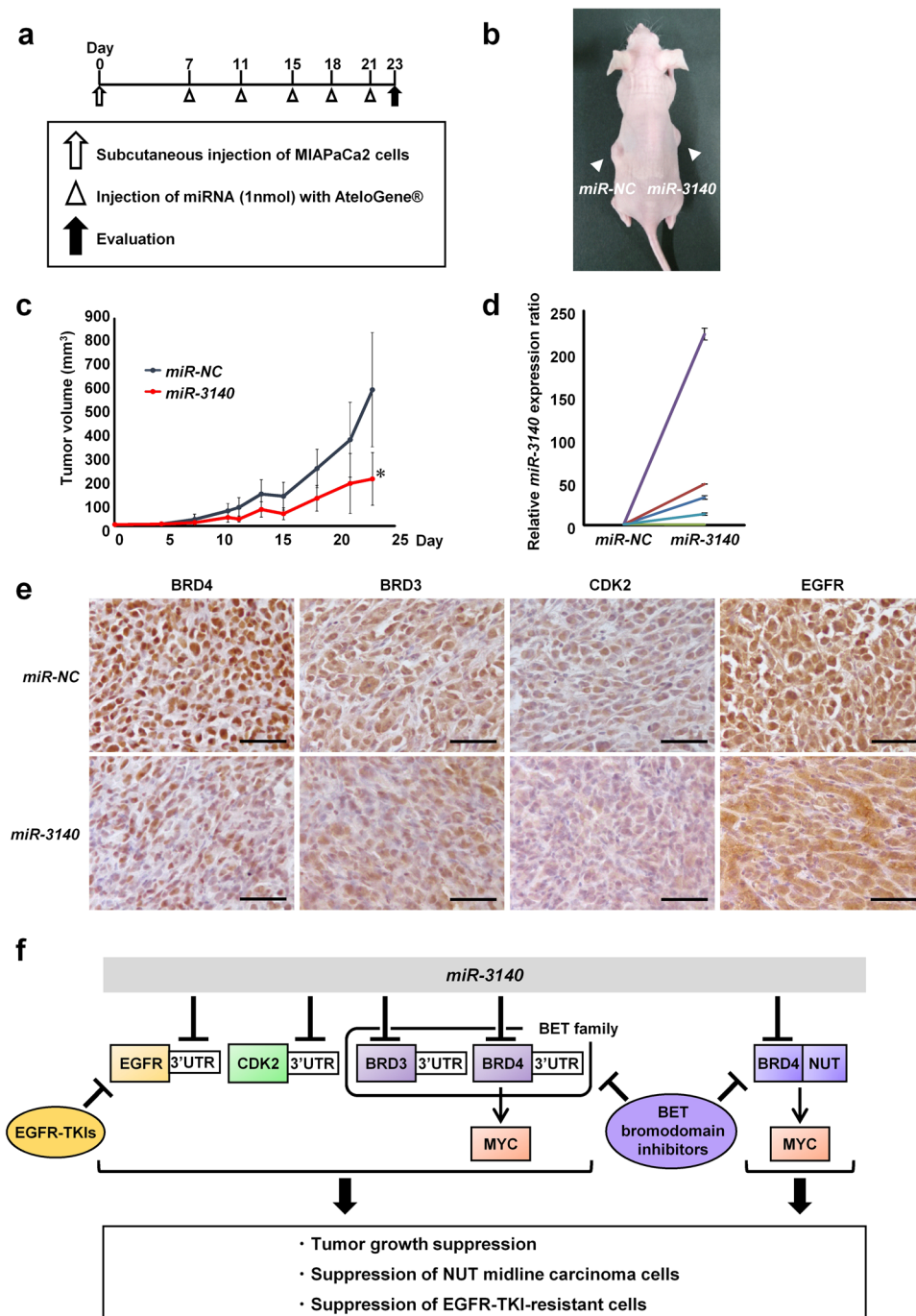


Figure 6. Therapeutic effects of *miR-3140* for tumor growth *in vivo*. (a) The experimental schedule for *miR-3140* treatment in nude mice which were subcutaneously inoculated with MIAPaCa2 cells. (b) The representative image of tumor-bearing nude mice at 23 days after the inoculation of MIAPaCa2 cells. Tumors are denoted by arrowheads. (c) Tumor growth curves of xenograft mouse models treated with *miR-NC* or *miR-3140* ($n = 5$, each). Tumor volume was calculated using the following formula: (shortest diameter) \times (longest diameter) \times 0.5. Bar, SD for 5 mice; * $P < 0.05$. (d) Expression analysis of *miR-3140* in resected tumors. The expression level of *miR-3140* was measured by qRT-PCR using the relative ratio normalized based on the expression of *RNU6B*. Each experiment was performed in duplicate. Bar, SD. (e) Representative images of immunohistochemical staining for BRD4, BRD3, CDK2 and EGFR in resected tumors. Scale bar, 50 μm . (f) Schematic models for the mechanism by which *miR-3140* suppresses tumor growth.

some cancers, including NMC^{16,24,25}. However, development of resistance to BET inhibition has been reported, in the same way as occurs in the other molecular targeted drugs. For example, BET inhibitor resistance is associated with increased BRD4 phosphorylation mediated by casein kinase 2 (CK2) in triple negative breast cancer cells⁸.

We showed that *miR-3140* suppressed the expression of BRD4-NUT in NMC cells. In the *BRD4-NUT* fusion gene, the translocation breakpoints of *BRD4* is within intron 10⁵⁰, and the binding sequence of *miR-3140* exists within exon 9 of *BRD4*. Thus, *miR-3140* can directly target the *BRD4-NUT* fusion gene and consequently, *miR-3140* suppressed *in vitro* tumor cell growth of Ty-82 cells as well as JQ1. Unfortunately, Ty-82 cells hardly formed subcutaneous tumors in our xenograft model. Further *in vivo* studies of the effect of *miR-3140* for NMC cells are needed for future work.

Our data suggested that *miR-3140* could suppress *in vitro* tumor cell growth of JQ1-resistant Ty-82 cells. Direct suppression of BRD4-NUT and concurrent downregulation of other tumor promoting genes such as *EGFR* and *CDK2* by *miR-3140* may potentially overcome resistance to BET inhibitors in NMC cells, although further studies are needed to clarify the acquired resistance of BET inhibitors. On the other hand, *miR-3140* might not suppress BRD3-NUT, since the translocation breakpoint of *BRD3* in *BRD3-NUT* fusion gene is within intron 9⁵¹, and the binding sequence of *miR-3140* exists within exon 10 of *BRD3*.

It was reported that the expression of BRD4 were increased by gemcitabine treatment in Panc1 and MIAPaCa2 cells, and the combination of BRD4 silencing and gemcitabine treatment had a synergistic effect on the chemotherapeutic efficacy⁵². A combined treatment of gemcitabine with *miR-3140* also may increase gemcitabine sensitivity in pancreatic cancer.

In primary samples, we did not observe a correlation between the expression levels of *miR-3140* and overall survival in pancreatic cancer, breast cancer, or acute myeloid leukemia according to the TCGA database (Supplementary Fig. S9a–c). This is because the *miR-3140* expression levels are very low in the majority of primary tumor samples, although *miR-3140* is predicted to exist in human tissue according to the miRBase database. Further investigation of the expression pattern of *miR-3140* in non-tumor tissues is required.

Because of recent advances in clinical tumor sequencing and developments in small molecule inhibitors, molecular targeted therapy is one of the key therapeutic strategies along with conventional chemotherapy, radiation therapy, and immunotherapy. However, acquired resistance to molecular targeted drugs is a major problem for cancer treatment⁴⁸. Reduction of the molecular target itself and other tumor promoting targets by a miRNA-based therapy may contribute to overcome the drug tolerance that develops against molecularly targeted drugs. In this study, our findings suggest that *miR-3140* suppresses tumor cell growth not only in various cancer cells, but also in EGFR-TKIs-resistant cells and JQ1-resistant cells. Although further *in vivo* studies of drug delivery systems and possible off-target effects are needed, *miR-3140* may be a candidate for the development of miRNA-based cancer therapeutics.

Materials and Methods

Cell culture. Panc1 and MIAPaCa2 cells were cultured in Dulbecco's Modified Eagle Medium containing 10% Fetal Bovine Serum (FBS). MDA-MB-231 cells from the American Type Culture Collection (Manassas, VA) were maintained in L-15 medium containing 10% FBS. KYSE150 cells, a gift from Dr. Shimada Y (Toyama University)⁵³, NCI-H1650, NCI-H1975, A549, HUT29 from ATCC, the NUT midline carcinoma cell line Ty-82 from JCRB, and 11–18 were maintained in RPMI1640 medium containing 10% FBS. The KYSE150 CDDP-resistant cell line (KYSE150 CDDP-R), which is resistant to cisplatin, was generated previously³⁶. Sk-Hep1 cells were maintained in Eagle's Minimum Essential Medium containing 10% FBS. All cell lines were maintained at 37 °C with 5% CO₂. The all experiments were carried out in accordance with the approved guidelines and regulations (2010-5-4, 2016-011C2).

Function-based miRNA screening. Two Panc1-derived clones (PEcadZsG-Panc1 #1 and #2 cells)³⁴ were seeded on 96-well plates. After 24 hours, each clone was transfected in duplicate with each of the 1090 dsRNAs from the Pre-miR miRNA Precursor Library-Human V15 (Thermo Fisher Scientific, CA) or a negative control miRNA (*miR-NC*) using an RNA concentration of 10 nmol/L. After 72 hours, viable cell number was assessed by the crystal violet staining assay. The results were normalized to the cell numbers of cells transfected with *miR-NC*.

Transfection of miRNAs and siRNAs. The dsRNA mimicking mature human *miR-3140-3p* (MC17496) and nonspecific control miRNA (negative control #1) were purchased from Thermo Fisher Scientific. The SMARTpool siRNA for *BRD2* (M-004935-02), *BRD3* (M-004936-01), *BRD4* (M-004937-02), *CDK2* (M-003236-04), *EGFR* (L-003114-00), nonspecific control siRNAs, and a set of 4 siRNA for *BRD4* (MQ-004937-02) were from GE Healthcare (Buckinghamshire, UK). Each SMARTpool siRNA consists of 4 siRNA duplexes designed to target different regions of the same gene. mRNA sequence. miRNAs and siRNAs were transfected individually into cells at the indicated concentrations using Lipofectamine RNAiMAX (Thermo Fisher Scientific) according to the manufacturer's instructions.

In vitro cell growth assay. The *in vitro* cell growth assay was carried out as described previously³⁴. Briefly, cell viability was measured using the WST-8 assay (Cell Counting Kit-8; Dojindo, Kumamoto, Japan) at the indicated number of days after plating, and the results were normalized to day 1 values. Each assay was carried out in triplicate.

Treatment with EGFR-TKI. Gefitinib and Erlotinib were purchased from Cayman Chemicals (Michigan, USA) and were resuspended in dimethyl sulfoxide (DMSO) to a final concentration of 100 mM and 500 mM for long-term storage, respectively. Cells were treated with the medium containing Gefitinib (0.001, 0.01, 0.1, 1, 5, 10, 25 μM), Erlotinib (0.001, 0.01, 0.1, 1, 5, 10, 25 μM), or DMSO for 72 hours. Cell viability was assessed by WST-8 assay as described above.

Gene expression array analysis. Gene expression array analysis was carried out as previously described³⁶. Briefly, Panc1, MIAPaCa2, and MDA-MB-231 cells were transfected with 10 nmol/L of miRNA (*miR-NC*, or

miR-3140). RNA was extracted 72 hours after transfection. The data were analyzed by GeneSpring software (Agilent Technologies, Japan).

Western blotting. Western blotting was performed according to previously reported methods³⁶. Primary antibodies for Western blotting were used as follows: antibodies for BRD4 (#13440), BRD2 (#5848), MYC (#9402), NUT (#3625), Cyclin D2 (#3741 S), p-STAT3 (#9145 S), STAT3 (#9139 S), and CDK6 (#3136) were purchased from Cell Signaling Technology; antibodies for CDK2 (sc-163) and EGFR (sc-03-G) from Santa Cruz Biotechnology; antibodies for BRD3 (A302-368A) from Bethyl Laboratories (Montgomery, TX); β -actin (A5441) and Vinculin (V9131) from Sigma-Aldrich (Tokyo, Japan); and HaloTag (G921A) from Promega (Tokyo, Japan).

Luciferase activity assay. Luciferase reporter plasmids were constructed by inserting the 3'UTR of *CDK2*, *EGFR* and CDS of *BRD4* and *BRD3* downstream of the luciferase gene within the pmirGLO Dual-Luciferase miRNA Target Expression Vector (Promega, Madison, WI, USA). All site-specific mutations used the KOD-Plus-Mutagenesis Kit (TOYOBO, Osaka, Japan). Luciferase reporter plasmids or control plasmid (pmirGLO) were transfected into Panc1 cells using Lipofectamine 2000 (Thermo Fisher Scientific), and 10 nmol/L of miRNA (*miR-NC* or *miR-3140*) was also transfected 6 hours later. After 2 days, Firefly and Renilla luciferase activities were measured using the Dual-Luciferase Reporter Assay System (Promega), and relative luciferase activity was calculated by normalizing the Firefly luciferase reading with its corresponding internal Renilla luciferase control.

Plasmid construction and transfection. BRD4 and BRD3 cDNA were purchased from Kazusa DNA Research Institute (Chiba, Japan) and were subcloned into the pFN28A HaloTag CMV-neo Flexi Vector (Promega, Madison, WI) to generate a mammalian expression vector. All site-specific mutations were generated using the KOD-Plus-Mutagenesis Kit (TOYOBO). The BRD3 or BRD4 expression vector or the empty vector were transfected into Panc1 and MIA PaCa2 cells using the Lipofectamine 2000 (Thermo Fisher Scientific), according to the manufacturer's instructions.

Establishment of JQ1-resistant cells. JQ1-resistant cells derived from Ty-82 were established by long-term incubation with gradually increasing JQ1 concentrations. JQ1 was purchased from APExBIO (Houston, TX). JQ1 was resuspended in DMSO to a final concentration of 10 mM for long-term storage. The cells were initially exposed to JQ1 at 0.1 μ mol/L in RPMI medium, then cultured in JQ1-free medium to confluence, and then exposed to JQ1 at a higher concentration. This cycle was repeated several times, until cells that were able to survive in RPMI medium including 2.5 μ mol/L JQ1 were defined as Ty-82 JQ1-R cells.

Real-time xCELLigence impedance analysis of cytotoxicity. Ty-82 cells and Ty-82 JQ1-R cells (3×10^4) were seeded in wells of the E-Plate 16 (ACEA Biosciences, San Diego, CA, USA). Approximately 48 hours later, these cells were treated with JQ1 (0.01, 0.05, 0.1, 0.5, 1, 5, 10 μ mol/L) (APExBIO) and DMSO. Cell-electrode impedance was monitored using the xCELLigence RTCA DP system (ACEA Biosciences) to produce time-dependent cell response dynamic curves. Data were collected every 5 min after treatment with JQ1 for the first four hours, every 15 min for the next 20 hours, and then every 1 hour for an additional 48 hours. Dose response curves of JQ1 for Ty-82 cells and Ty-82 JQ1-R cells at 50 hours following treatment with JQ1 were constructed. Cell indexes were normalized with the last time point before treatment with JQ1.

In vivo tumor growth and miRNA administration. *In vivo* miRNA administration of miRNA was performed as previously described³⁶. Six-week-old female BALB/c nude mice were purchased from Oriental Bio Service, Japan. Briefly, a total of 5.0×10^6 cells in 100 μ L of PBS were subcutaneously injected into the dorsal side of the mice. After tumor formation at day 7, a mixture of 1 nmol dsRNA (*miR-NC* or *miR-3140*) and 100 μ L AteloGene (KOKEN, Tokyo, Japan) was administered around the tumor (*miR-NC* to the left dorsal side and *miR-3140* to the right dorsal side of mice). miRNAs were administered on days 7, 11, 15, 18, and 21, and at 23 days after cell injection, mice were sacrificed and tumors were resected. Tumor volume was calculated using the following formula: (shortest diameter)² \times (longest diameter) \times 0.5. All experimental protocols conducted on the mice were approved by the Tokyo Medical and Dental University Animal Care and Use Committee.

Immunohistochemistry. Immunohistochemistry was performed as previously described⁵⁴. The resected tumors from xenograft mouse model were fixed in 10% formaldehyde in PBS for 24 h and stored in 70% ethanol and then embedded in paraffin. The following primary antibodies were used for immunohistochemistry: an antibody for BRD4 (HPA061646, 1:500) was purchased from Atlas Antibodies (Stockholm, Sweden), BRD3 (A302-368A, 1:500) and CDK2 (IHC-00374, 1:500) antibodies were from Bethyl Laboratories, and EGFR (sc-03-G, 1:200) antibody was from Santa Cruz Biotechnology (Santa Cruz, CA). BRD4, BRD3, EGFR, and CDK2 staining were scored semiquantitatively using histo-score (H-score) based on staining intensity and percentage of positive cells. Staining intensity was scored as follows: 0 = none, 1 = weak, 2 = moderate, or 3 = strong. H-score was calculated by multiplying the intensity of staining with percentage of cells stained in randomly chosen 3 fields from each specimen⁵⁵.

Quantitative RT-PCR (qRT-PCR). Total RNA was extracted using TRIreagent (BIOLINE, London, UK) according to the manufacturer's instructions. For miRNA, total RNA was reverse transcribed using the Taqman Reverse Transcription Kit followed by qRT-PCR performed using Custom Taqman miRNA Assays (Applied Biosystems, Foster City, CA). The miRNA expression was normalized to the internal control *RNU6B*. The following primers were used for the Taqman assay (Thermo Fisher Scientific): human *miR-3140-3p* (244524), *RNU6B* (001093).

Public datasets. To explore the generality of the miRNA expression and clinical features among pancreatic cancer, breast cancer and acute myeloid leukemia (AML), we examined the public datasets from TCGA (<http://cancergenome.nih.gov>) retrieved on 24th July 2017. We used TCGA datasets on primary cases for pancreatic cancer, breast cancer and AML, and examined correlation of prognosis and expression of *miR-3140*. The datasets we used included mRNA-expression data on 174 samples of pancreatic cancer, 972 samples of breast cancer, 89 samples of AML and 1881 miRNAs, respectively.

Statistical analysis. Student's *t*-test, Paired *t*-test and log-rank test were performed using R software. P values of < 0.05 were considered significant.

Ethical Approval. All experimental protocols conducted on the mice were approved by the Tokyo Medical and Dental University Animal Care and Use Committee (0170036C).

References

- Belkina, A. C. & Denis, G. V. BET domain co-regulators in obesity, inflammation and cancer. *Nat. Rev. Cancer* **12**, 465–477 (2012).
- Fujisawa, T. & Filippakopoulos, P. Functions of bromodomain-containing proteins and their roles in homeostasis and cancer. *Nat. Rev. Mol. Cell Biol.* **18**, 246–262 (2017).
- Zuber, J. *et al.* RNAi screen identifies Brd4 as a therapeutic target in acute myeloid leukaemia. *Nature* **478**, 524–528 (2011).
- Blobel, G. A., Kalota, A., Sanchez, P. V. & Carroll, M. Short hairpin RNA screen reveals bromodomain proteins as novel targets in acute myeloid leukemia. *Cancer Cell* **20**, 287–288 (2011).
- Delmore, J. E. *et al.* BET bromodomain inhibition as a therapeutic strategy to target c-Myc. *Cell* **146**, 904–917 (2011).
- Dawson, M. *et al.* Inhibition of BET recruitment to chromatin as an effective treatment for MLL-fusion leukaemia. *Nature* **478**, 529–533 (2011).
- Chapuy, B. *et al.* Discovery and Characterization of Super-Enhancer-Associated Dependencies in Diffuse Large B Cell Lymphoma. *Cancer Cell* **24**, 777–790 (2013).
- Shu, S. *et al.* Response and resistance to BET bromodomain inhibitors in triple-negative breast cancer. *Nature* **529**, 413–417 (2016).
- Sahai, V. *et al.* BET Bromodomain Inhibitors Block Growth of Pancreatic Cancer Cells in Three-Dimensional Collagen. *Mol. Cancer Ther.* **13**, 1907–1917 (2014).
- Lovén, J. *et al.* Selective inhibition of tumor oncogenes by disruption of super-enhancers. *Cell* **153**, 320–334 (2013).
- Sun, B. *et al.* Synergistic activity of BET protein antagonist-based combinations in mantle cell lymphoma cells sensitive or resistant to ibrutinib. *Blood* **126**, 1565–1574 (2015).
- French, C. A. Demystified molecular pathology of NUT midline carcinomas. *J. Clin. Pathol.* **63**, 492–6 (2010).
- French, C. NUT midline carcinoma. *Nat. Rev. Cancer* **14**, 149–50 (2014).
- French, C. A. *et al.* NSD3-NUT fusion oncoprotein in NUT midline carcinoma: Implications for a novel oncogenic mechanism. *Cancer Discov.* **4**, 929–941 (2014).
- Alekseyenko, A. A. *et al.* Ectopic protein interactions within BRD4–chromatin complexes drive oncogenic megadomain formation in NUT midline carcinoma. *Proc. Natl. Acad. Sci.* **114**, E4184–E4192 (2017).
- Stathis, A. *et al.* Clinical response of carcinomas harboring the BRD4–NUT oncoprotein to the targeted bromodomain inhibitor OTX015/MK-8628. *Cancer Discov.* **6**, 492–500 (2016).
- Wang, R. & You, J. Mechanistic analysis of the role of bromodomain-containing protein 4 (BRD4) in BRD4-NUT oncoprotein-induced transcriptional activation. *J. Biol. Chem.* **290**, 2744–2758 (2015).
- Reynoird, N. *et al.* Oncogenesis by sequestration of CBP/p300 in transcriptionally inactive hyperacetylated chromatin domains. *EMBO J.* **29**, 2943–2952 (2010).
- Wang, R. *et al.* Activation of SOX2 expression by BRD4-NUT oncogenic fusion drives neoplastic transformation in NUT midline carcinoma. *Cancer Res.* **74**, 3332–3343 (2014).
- Mazur, P. K. *et al.* Combined inhibition of BET family proteins and histone deacetylases as a potential epigenetics-based therapy for pancreatic ductal adenocarcinoma. *Nat. Med.* **21**, 1163–71 (2015).
- Ott, C. J. *et al.* BET bromodomain inhibition targets both c-Myc and IL7R in high-risk acute lymphoblastic leukemia. *Blood* **120**, 2843–2852 (2012).
- Filippakopoulos, P. *et al.* Selective inhibition of BET bromodomains. *Nature* **468**, 1067–73 (2010).
- Rathert, P. *et al.* Transcriptional plasticity promotes primary and acquired resistance to BET inhibition. *Nature* **525**, 543–547 (2015).
- Berthon, C. *et al.* Bromodomain inhibitor OTX015 in patients with acute leukaemia: A dose-escalation, phase 1 study. *Lancet Haematol.* **3**, e186–e195 (2016).
- Amorim, S. *et al.* Bromodomain inhibitor OTX015 in patients with lymphoma or multiple myeloma: A dose-escalation, open-label, pharmacokinetic, phase 1 study. *Lancet Haematol.* **3**, e196–e204 (2016).
- Wang, C. Y. & Filippakopoulos, P. Beating the odds: BETs in disease. *Trends Biochem. Sci.* **40**, 468–479 (2015).
- Lin, S. & Gregory, R. I. MicroRNA biogenesis pathways in cancer. *Nat. Rev. Cancer* **15**, 321–333 (2015).
- Iorio, M. V. & Croce, C. M. MicroRNA dysregulation in cancer: Diagnostics, monitoring and therapeutics. A comprehensive review. *EMBO Mol. Med.* **4**, 143–159 (2012).
- Forman, J. J., Legesse-Miller, A. & Collier, H. A. A search for conserved sequences in coding regions reveals that the let-7 microRNA targets Dicer within its coding sequence. *Proc. Natl. Acad. Sci. USA* **105**, 14879–84 (2008).
- Hausser, J., Syed, A. P., Bilén, B. & Zavolan, M. Analysis of CDS-located miRNA target sites suggests that they can effectively inhibit translation. *Genome Res.* **23**, 604–615 (2013).
- Ito, Y. *et al.* Identification of targets of tumor suppressor microRNA-34a using a reporter library system. *Proc. Natl. Acad. Sci.* **114**, 3927–3932 (2017).
- Akdemir, B., Nakajima, Y., Inazawa, J. & Inoue, J. *miR-432* Induces NRF2 Stabilization by Directly Targeting KEAP1. *Mol. Cancer Res. molcanres.* **0232**, 2017, <https://doi.org/10.1158/1541-7786.MCR-17-0232> (2017).
- Kong, Y. W., Ferland-McCollough, D., Jackson, T. J. & Bushell, M. MicroRNAs in cancer management. *Lancet Oncol.* **13**, e249–e258 (2012).
- Hiramoto, H. *et al.* miR-509-5p and miR-1243 increase the sensitivity to gemcitabine by inhibiting epithelial-mesenchymal transition in pancreatic cancer. *Sci. Rep.* **7**, 4002 (2017).
- Yang, H. *et al.* microRNA-342-5p and miR-608 inhibit colon cancer tumorigenesis by targeting NAA10. *Oncotarget* **7**, 2709–2720 (2016).
- Fujiwara, N. *et al.* miR-634 activates the mitochondrial apoptosis pathway and enhances chemotherapy-induced cytotoxicity. *Cancer Res.* **75**, 3890–3901 (2015).
- Warnecke-Eberz, U., Chon, S. H., Hölscher, A. H., Drebber, U. & Bollschweiler, E. Exosomal onco-miRs from serum of patients with adenocarcinoma of the esophagus: comparison of miRNA profiles of exosomes and matching tumor. *Tumor Biol.* **36**, 4643–4653 (2015).

38. Tréhoux, S. *et al.* Micro-RNAs miR-29a and miR-330-5p function as tumor suppressors by targeting the MUC1 mucin in pancreatic cancer cells. *Biochim. Biophys. Acta - Mol. Cell Res.* **1853**, 2392–2403 (2015).
39. Kozomara, A. & Griffiths-Jones, S. MiRBase: Annotating high confidence microRNAs using deep sequencing data. *Nucleic Acids Res.* **42**, 68–73 (2014).
40. Du, J. *et al.* Critical role of CDK2 for melanoma growth linked to its melanocyte-specific transcriptional regulation by MITF. *Cancer Cell* **6**, 565–576 (2004).
41. Asghar, U., Witkiewicz, A. K., Turner, N. C. & Knudsen, E. S. The history and future of targeting cyclin-dependent kinases in cancer therapy. *Nat. Rev. Drug Discov.* **14**, 130–146 (2015).
42. Gazdar, A. F. & Minna, J. D. Deregulated EGFR signaling during lung cancer progression: Mutations, amplicons, and autocrine loops. *Cancer Prev. Res.* **1**, 156–160 (2008).
43. Sharma, S. V., Bell, D. W., Settleman, J. & Haber, D. A. Epidermal growth factor receptor mutations in lung cancer. *Nat. Rev. Cancer* **7**, 169–181 (2007).
44. Rennie, W. *et al.* STarMirDB: A database of microRNA binding sites. *RNA Biol.* **13**, 554–60 (2016).
45. Grayson, aR. *et al.* MYC, a downstream target of BRD-NUT, is necessary and sufficient for the blockade of differentiation in NUT midline carcinoma. *Oncogene* **33**, 1–7 (2013).
46. Kuzume, T. *et al.* Establishment and characterization of a thymic carcinoma cell line (Ty-82) carrying t(15;19)(q15; p13) chromosome abnormality. *Int. J. Cancer J. Int. du cancer* **50**, 259–264 (1992).
47. Ke, E. E. & Wu, Y. L. EGFR as a Pharmacological Target in EGFR-Mutant Non-Small-Cell Lung Cancer: Where Do We Stand Now? *Trends Pharmacol. Sci.* **37**, 887–903 (2016).
48. Politi, K., Ayeni, D. & Lynch, T. The Next Wave of EGFR Tyrosine Kinase Inhibitors Enter the Clinic. *Cancer Cell* **27**, 751–753 (2015).
49. Otto, T. & Sicinski, P. Cell cycle proteins as promising targets in cancer therapy. *Nat. Rev. Cancer* **17**, 93–115 (2017).
50. French, C. A. *et al.* BRD4-NUT Fusion Oncogene: A Novel Mechanism in Aggressive Carcinoma Advances in Brief BRD4-NUT Fusion Oncogene: A Novel Mechanism in Aggressive Carcinoma 1. *Cancer Res.* **63**, 304–307 (2003).
51. French, C. A. *et al.* BRD-NUT oncoproteins: a family of closely related nuclear proteins that block epithelial differentiation and maintain the growth of carcinoma cells. *Oncogene* **27**, 2237–2242 (2008).
52. Wang, Y. H. *et al.* BRD4 promotes pancreatic ductal adenocarcinoma cell proliferation and enhances gemcitabine resistance. *Oncol. Rep.* **33**, 1699–1706 (2015).
53. Shimada, Y., Imamura, M., Wagata, T., Yamaguchi, N. & Tobe, T. Characterization of 21 newly established esophageal cancer cell lines. *Cancer* **69**, 277–284 (1992).
54. Endo, H. *et al.* Potential of tumor-suppressive miR-596 targeting LGALS3BP as a therapeutic agent in oral cancer. *Carcinogenesis* **34**, 560–569 (2013).
55. Lessey, B. A. *et al.* Immunohistochemical analysis of human uterine estrogen and progesterone receptors throughout the menstrual cycle. *J. Clin. Endocrinol. Metab.* **67**, 334–40 (1988).

Acknowledgements

We thank Ayako Takahashi and Rumi Mori for technical assistance. This work was supported by KAKENHI (15H05908, 16K14630, 15K18401, 15K19040) from the Ministry of Education, Culture, Sports, Science, and Technology (MEXT), and partially supported by the Project for Cancer Research And Therapeutic Evolution (P-CREATE) from Japan Agency for Medical Research and development, AMED. This study was also partly supported by Nanken-Kyoten, TMDU.

Author Contributions

E. Tonouchi, and Y. Gen were involved in research design, performed the experiments, analyzed data and wrote the manuscript. T. Muramatsu and H. Hiramoto were involved in research design, performed the experiments, and analyzed data. K. Tanimoto contributed to TCGA data analysis. J. Inoue contributed materials. J. Inazawa was involved in research design, wrote the manuscript, and study supervision.

Additional Information

Supplementary information accompanies this paper at <https://doi.org/10.1038/s41598-018-22767-y>.

Competing Interests: The authors declare no competing interests.

Publisher's note: Springer Nature remains neutral with regard to jurisdictional claims in published maps and institutional affiliations.



Open Access This article is licensed under a Creative Commons Attribution 4.0 International License, which permits use, sharing, adaptation, distribution and reproduction in any medium or format, as long as you give appropriate credit to the original author(s) and the source, provide a link to the Creative Commons license, and indicate if changes were made. The images or other third party material in this article are included in the article's Creative Commons license, unless indicated otherwise in a credit line to the material. If material is not included in the article's Creative Commons license and your intended use is not permitted by statutory regulation or exceeds the permitted use, you will need to obtain permission directly from the copyright holder. To view a copy of this license, visit <http://creativecommons.org/licenses/by/4.0/>.

© The Author(s) 2018